Research Paper

Bufrudin Reduces Atherosclerosis in Apolipoprotein E Knockout Mice by Modulating the Toll-Like Receptor 4/ Nuclear Factor Kappa B/p38 Mitogen-Activated Protein Kinase Signalling Pathway in the Aorta

JIXING LI, WENXING WEI, SI LIN, WENWEN TAN, ZONGQIANG LAI, YU TU1 AND YUANHONG LI*

Department of Pharmacy, Second Affiliated Hospital of Guangxi Medical University, Nanning 530007, China

Li *et al.*: Effects and Mechanisms of Bufrudin in Inhibiting Atherosclerosis

Atherosclerosis is a significant cause of cardiovascular disease morbidity and mortality worldwide, seriously threatening human health and life. Therefore, the present study aimed to investigate the effects and mechanisms of Bufrudin in inhibiting atherosclerosis. The atherosclerosis model was induced using high-fat diet-fed apolipoprotein E knockout mice, which were fed a high-fat diet for 8 w and subsequently intraperitoneally injected with Bufrudin for 8 w; rosuvastatin was used as the positive group. Serum lipid levels, atherosclerotic lesion area and levels of related inflammatory factors were detected in mice, and the mechanism of the anti-atherosclerotic effect of Bufrudin was investigated by reverse transcription-quantitative polymerase chain reaction protein immunoblotting and immunohistochemistry. The results showed that similar to rosuvastatin, Bufrudin reduced serum cholesterol, low-density lipoprotein cholesterol and triglyceride levels, and increased high-density lipoprotein cholesterol levels in mice. Meanwhile, Bufrudin reduced the area of atherosclerotic lesions, increased the collagen content in atherosclerotic plaques and lowered the levels of interleukin-6, tumour necrosis factor-alpha and C-reactive protein in mice. In addition, Western blotting results showed that Bufrudin downregulated the expression of cellular myelocytomatosis oncogene, mitogen-activated protein kinase 3 and p38 proteins. Furthermore, reverse transcription-quantitative polymerase chain reaction and immunohistochemistry results showed that Bufrudin downregulated the expression of cluster of differentiation 36, tumour necrosis factor-alpha, toll-like receptor 4 and myeloid differentiation primary-response protein 88 messenger ribonucleic acid and proteins in mice. In conclusion, Bufrudin ameliorated atherosclerosis in apolipoprotein E knockout mice by mechanisms related to the improvement of serum lipid levels, inflammatory factor levels and with the inhibition of the toll-like receptor 4/nuclear factor kappa B and p38 mitogen-activated protein kinase pathways. The results revealed a novel anti-atherosclerosis mechanism of Bufrudin, which lays a foundation for its clinical use in modulating atherosclerosis.

Key words: Bufrudin, atherosclerosis, serum lipid, inflammation, toll-like receptor 4/nuclear factor kappa B pathway, p38 mitogen-activated protein kinase pathway

Cardiovascular Diseases (CVDs) include myocardial infarction, heart failure, ischemic heart disease, stroke and limp[1]. According to the World Health Organization (WHO), >17 million individuals die from CVDs annually, accounting for 32 % of global mortalities[2]. Atherosclerosis (AS) is the leading cause of CVDs. Therefore, the WHO regards CVD-based on AS a paramount human health concern and lists it as a severe global social issue that must be solved urgently[2].

The production of AS is related to numerous factors, including oxidative stress, lipid infiltration, injury response, monocyte-macrophage invasion and inflammatory response[3]. The clinical treatment of AS is mainly cardiovascular interventional therapy and receiving statins, but this only treats the downstream effects of AS, and has limitations

***Address for correspondence**
E-mail: zyli2007@163.com

Accepted 21 August 2024
Revised 20 December 2023
Received 26 May 2023
Indian J Pharm Sci 2024;86(4):1521-1534

regarding efficacy and adverse reactions. Currently, the clinical treatment of AS is mainly statins, and although some effects have been achieved, it still has not had any impact on the high incidence levels of AS. Furthermore, statins are associated with adverse reactions such as myalgia, myositis, rhabdomyolysis and liver injury[4,5], and notably, an increased risk of hemorrhagic stroke[6,7]. Therefore, the urgent search for a highly effective drug treatment for AS with minimal or no side effects is imperative.

Vascular endothelium with normal structure and function ensure the homeostasis of blood vessels, maintain blood flow, regulate vascular tension and anti-inflammatory effects, and are considered the first line of defines against AS[1]. Vascular endothelial cells are highly selective[8], and can synthesize and release various vasoactive factors. These substances antagonize each other to maintain a dynamic balance between pro-AS and anti-AS[9]. Inflammation is vital in all stages of AS development[10]. Tumour Necrosis Factor-Alpha (TNF-α) is an inflammatory cytokine that plays a central role in immune and inflammatory responses and is a significant circulating substance, linking the systemic immune response to local vascular injury; TNF-α and other pro-inflammatory cytokines, which are often present in AS plaques [11]. C-Reactive Protein (CRP) is considered one of the most essential inflammatory markers of acute cardiovascular events. It is synthesized in the liver induced by Interleukin (IL)-6, IL-1β and TNF-α, which activate apoptosis, leukocyte recruitment, lipid accumulation and platelet aggregation by activating the complement system, ultimately leading to thrombus formation. IL-6 increases the platelet count in peripheral vasculature, induces thrombocytosis, participates in vascular monocyte differentiation, and is associated with obesity and metabolism. In addition, it induces monocyte tissue factor expression while enhancing its procoagulant activity, leading to a sustained loss of endothelial barrier function and destabilization of AS plaques.

Lipid-rich foam cells are a marker of atherosclerotic plaques[12]. A number of studies have shown that lipid accumulation can induce macrophages to transform into harmful foam cells[13-16]. For example, phagocytic-modified lipids such as scavenger receptor Cluster of Differentiation (CD) 36 (such as oxidized Low Density Lipoprotein (ox-LDL)) can form foam cells in macrophages[17], thus accelerating the instability, rupturing and thrombosis of AS plaques[18]. Furthermore, the activation of Toll-like receptor 4 (TLR4) also promotes ox-LDL uptake by macrophages, thereby accelerating the formation of foam cells. The expression of Nuclear Factor Kappa B (NF-κB) is involved in macrophages and Vascular Smooth Muscle Cells (VSMC), and its relative expression is related to the early development of AS. The NF-κB pathway intervenes in the progression of AS by transcriptionally activating the production of pro-inflammatory cytokines and chemokines, such as TNF-α, the Granulocyte-Macrophage Colony-Stimulating Factor (GM-CSF) and IL-1, promoting the generation of an inflammatory milieu. TLR4 also mediates the NF-κB pathway and thus affects Total Cholesterol (TC) metabolism. Activation, migration and proliferation of VSMC are critical components of the pathological process of AS[19]. p38 Mitogen-Activated Protein Kinase (MAPK) is an important pathway that regulates cell proliferation and death and plays an important role in various physio pathological processes, including inflammation, stress, cell proliferation, differentiation and apoptosis[20]. Therefore, the TLR4/NF-κB and p38 MAPK signalling pathways are crucial for the development of AS.

Bufrudin is an active substance extracted from traditional Chinese medicinal leeches, which are native to Guangxi and belong to the family of water leeches. The active extract of leeches, termed hirudin, has been approved by the United States of America (USA) Food and Drug Administration and is widely used for the treatment of CVDs. Bufrudin was included in the Guangxi Zhuang medicine catalogue in 2011[21]. It is a natural anticoagulant extracted from *Poecilobdella manillensis* (*P. manillensis*), with the extraction method adhering to the requirements of the Pharmacopoeia of the People's Republic of China (2020 edition). Our research group cloned and sequenced the complementary Deoxyribonucleic Acid (cDNA) of the Bufrudin gene and found that the Homology Model (HM) 1 and HM2 gene sequences of Guangxi *P. manillensis* and Manila *P. manillensis* were 91.8 % and 84.7 %, respectively[22]. The study of Bufrudin has proven that it has beneficial effects on the cardiovascular system. Previous studies have reported that Bufrudin can inhibit arterial thrombosis and reduce arterial wall inflammation[23,24]. Our previous studies provided a preliminary understanding of the anti-AS effect of Bufrudin[25,26]. However, the specific mechanism of the anti-AS effect of Bufrudin remains unclear. Similarly, whether Bufrudin can alleviate AS by inhibiting the TLR4/NF-κB/p38

MAPK signalling pathway is still unknown.

Therefore, the aim of the present study was to investigate whether Bufrudin can achieve the effect of anti-AS by affecting the TLR4/NF-κB/p38 MAPK pathway and to provide new insights into the mechanism of Bufrudin against AS, thus providing a reference for the development of clinical drugs for the treatment of AS.

MATERIALS AND METHODS

Reagents:

Bufrudin (40 U/ml) was supplied by Guangxi Keyken Technology Group Co. Ltd., and rosuvastatin tablets (10 mg/tablet) were purchased from AstraZeneca Co. Ltd., the high-fat feed was purchased from Nanjing Qingzilan Technology Co. Ltd., kits to assess levels of low-density lipoprotein cholesterol (cat. no. A113-1-1), high-density lipoprotein cholesterol (cat. no. A112-1-1), TC (cat. no. A111-1-1) and triglycerides (cat. no. A110-1-1) were from Nanjing Jiancheng Bioengineering Institute. Enzyme-Linked Immunosorbent Assay (ELISA) kits for CRP (cat. no. F2074-B), IL-6 (cat. no. F2163-B) and TNF-α (cat. no. F2132-B) were from Shanghai Kexing Fanke Group Co. Ltd., Mouse β-actin was purchased from Abcam (dilution, 1:6,000; cat. no. ab8245), rabbit anti-MAK3, (dilution, 1:2000; cat. no. 13898-1-AP), anti-Cellular Myelocytomatosis Oncogene (c-MYC) (dilution, 1:5000; cat. no. 10828-1-AP) and anti-TLR4 (dilution, 1:200; cat. no. 19811-1-AP) were purchased from Proteintech, rabbit anti-P38 (dilution, 1:2000; cat. no. A10832) and anti-NF-κB (dilution, 1:100; cat. no. A17339) were purchased from ABclonal, rabbit anti-Myeloid Differentiation Primary-Response Protein 88 (MYD88) (dilution, 1:200; cat. no. bs-1047R) and anti-CD36 (dilution, 1:200; cat. no. bs-0465R) were purchased from Boson, Horseradish Peroxidase (HRP)-goat anti rabbit (dilution, 1:50 000; cat. no. 5220-0336) and HRP-goat anti mouse (dilution, 1:50 000; cat. no. 5220-0341) were purchased from Searcare and PCR primers were purchased from Sangon Biotech Shanghai Co. Ltd.,.

Animal model establishment and drug administration:

Apolipoprotein E Knockout (ApoE-/-) male mice (18±2 g; 8 w old) and C57BL/6J mice (body weight, 18±2 g; 8 w old) were purchased from Nanjing Qing Zilan Science and Technology Co., Ltd and housed in the Laboratory Animal Management Canter of Guangxi Medical University (Nanning, China; approval no. SYXK Gui 2020-0004), at a temperature of 20°-24° and humidity of 40 %-60 %, with a 12 h light/dark cycle. C57BL/6J mice were given free access to standard laboratory mouse chow and drinking water, whereas the ApoE-/- mice were given free access to high-fat chow and drinking water. To establish an AS model, ApoE-/- mice were fed a high-fat diet (consisting of a normal diet containing 0.5 % TC and 5 % lard) for 8 w. Mice were randomly divided into four groups according to body weight: High-dose Bufrudin group, low-dose Bufrudin group, rosuvastatin group and model group, with C57BL/6J mice used as the control group. In the high-dose and low-dose Bufrudin groups, Bufrudin 400 U/kg/d and 200 U/kg/d were administered intraperitoneally for 8 w, while in the positive group, rosuvastatin 2.5 mg/kg/d was administered by gavage. The model group and the blank group were administered an equal amount of normal saline. The mice were anesthetized with isoflurane (1.5 %) until they were unconscious, during which time the blood sample was taken from the abdominal aorta, and then sacrificed the mice *via* decapitation. After that, the sampling steps of abdominal aorta and thoracic aorta were performed. All experiments were approved by The Animal Care & Welfare Committee of Guangxi Medical University, which followed the guidelines of the National Standard GB/T35892-2018 of the People's Republic of China.

Determination of blood lipid content:

The serum was isolated from blood samples at 1000 rpm for 10 min at 4°, and the levels of serum TC, LDL-C, HDL-C and TG in each group were determined using kits according to the manufacturer's instructions.

Oil Red O (ORO) staining:

Cardiac tissue samples with aortic roots were fixed with 4 % paraformaldehyde (pH 7.4), dehydrated in alcohol and embedded in the Tissue Tek® O.C.T. Compound. After which, the tissues were sectioned at a thickness of ~10 μm with a frozen sectioning machine, and the sections were stained with ORO to determine the morphology of atherosclerotic plaques. Morphometric analysis was performed using Image J software (1.8.0, National Institutes of Health, NIH, Bethesda, MD, USA).

Masson's trichrome stain:

Masson's trichrome stain was performed to detect the collagen content in the aortic root plaques. According to the manufacturer's instructions, the aorta was fixed in 4 % paraformaldehyde, dehydrated in alcohol, embedded

in paraffin wax, sectioned and stained, observed and images were captured under a light microscope. The percentage area of collagen in the plaques was calculated using the Image J assay.

ELISA for quantitative analysis of mice serum inflammatory indexes:

The concentrations of IL-6, TNF-α and CRP in the serum of mice were detected according to the instructions of the ELISA kit.

Western blot analysis:

Western blotting was used to detect the protein levels of c-MYC, MEK3, and p38 MAPK in the thoracic aorta of mice. The aorta of each group of mice was homogenized using a refrigerated centrifuge homogenizer, and Radio-Immunoprecipitation Assay (RIPA) buffer was added for lysis and mixing. After centrifugation, the supernatant was collected, and the protein concentration of the sample was determined using a Bicinchoninic Acid (BCA) protein concentration assay kit. Electrophoresis was performed according to standard electrophoresis procedures and the membrane was transferred. After which, the membrane was removed and placed in a blocking solution at 37° for 1 h. The following primary antibodies were added: c-MYC (1:5 000), MEK3 (1:5000) and p38 MAPK (1:2000) at 4° overnight. The HRP-gGoat anti rRabbit (1:50,000) was incubated after washing the membrane repeatedly, and then gently agitated at room temperature for 1 h. The samples were washed three times for colour development and exposure. Image Jwas used to calculate the grayscale of the target protein band and analyse the relative protein expression.

Reverse Transcription-quantitative Polymerase Chain Reaction (RT-qPCR):

RT-qPCR was performed to detect the expression levels of CD36, TNF-α, TLR4 and MyD88 messenger Ribonuclic Acid (mRNA) in the aortas of mice in each group. The aortas of each group were homogenized with Trizol in a freezing centrifuge homogenizer, and the supernatant was centrifuged. The supernatant was mixed with trichloromethane and centrifuged again. The sample was mixed with isopropanol and centrifuged for a third time and the liquid was discarded. The precipitate was washed twice with 75 % ethanol, and finally, the RNA was dissolved in RNA-free water. The concentration and purity of RNA were analysed by ultra-micro spectrophotometer. The cDNA was synthesized by PCR using a 20 µl reverse transcription system, and the mRNA levels of each inflammatory mediator were detected by qPCR using SYBR Green qPCR Master Mix. Glyceraldehyde 3-Phosphate Dehydrogenase (GAPDH) was used as the internal reference, and the relative expression values of each factor, including CD36, TNF-α, TLR4 and MyD88, in each group was calculated by the $2^{-\Delta\Delta Cq}$ method. The primers used are shown in Table 1.

TABLE 1: PRIMERS USED FOR RT-qPCR

Gene	Primer	Sequence 5-3′
GAPDH	Forward primer	CCTCGTCCCGTAGACAAAATG
GAPDH	Reverse primer	TGAGGTCAATGAAGGGGTCGT
CD36	Forward primer	CCCAGAGTACGGGCAAAGA
CD36	Reverse primer	TCCAACAGACAGTGAAGGCTCAA
TLR4	Forward primer	TCCTGTGGACAAGGTCAGCAAC
TLR4	Reverse primer	TTACACTCAGACTCGGCACTTAGCA
MyD88	Forward primer	TACAGGTGGCCAGAGTGGAA
MyD88	Reverse primer	GCAGTAGCAGATAAAGGCATCGAA
NF-kB	Forward primer	GAGGGTTGGGAGAATGTGGA
NF-kB	Reverse primer	GGAAGCAGAAAGAACGGAAGG

Immunohistochemistry:

Immunohistochemistry was used to measure the expression of CD36, TNF-α, TLR4 and MyD88 proteins. The sections were heated at 65° for 30 min; after which, the sections were deparaffinized by xylene and alcohol and repaired by selecting the appropriate antigen repair solution according to the instructions of the antibody. The sections were washed with Phosphate Buffer Solution (PBS), and stained according to the instructions of the immunohistochemistry kit. Following intervention of blocking peroxidase and serum closure, the sections were washed by PBS, and rabbit anti-CD36 (1:200), anti-TNF-α (1:200), anti-TLR4 (1:200) and anti-MyD88 (1:200) were added. The sections were incubated with primary antibodies at 4° overnight, and subsequently the The HRP-gGoat anti rRabbit (1:500) was added. 3, 3'-Diaminobenzidine (DAB) chromogenic solution was added after the antibody incubation and the samples were protected from light. Hematoxylin was used for counterstaining after washing and the staining was decolorized, reversed to blue and sealed. Sections were observed under the microscope and images were captured.

Statistical analysis:

All data were expressed as the mean±standard deviation. Continuous data with normal distribution were displayed as mean±standard deviation (x±s). Statistical Package for the Social Sciences (SPSS) 25.0 statistical program package for Windows (SPSS Inc., Chicago, IL, USA) was adopted for statistical analysis. Categorical data were expressed as composition ratios and analysed using the Chi-Square ($\chi 2$) test. Normally distributed and non-normally distributed continuous data were represented as mean±standard deviation ($\bar{x}$±s) and median (Q1, Q3), respectively, and analysed using the t-test and Kruskal-Wallis rank sum test. One-way Analysis of Variance (ANOVA) was conducted for data that met the criteria for normal distribution and homogeneity of variance, with pairwise comparisons between groups performed using the Tukey test. For comparisons involving multiple time points, repeated measures ANOVA was used. If the assumptions were not met, variable transformation or analysis using the Generalized Estimating Equation (GEE) was performed. $p<0.05$ was considered to indicate a statistically significant difference.

RESULTS AND DISCUSSION

The expression of serum TC, TG and LDL-C in ApoE-/- mice in each group was shown in fig. 1A-fig. 1D. Compared with the control group, the levels of TC, TG and LDL-C were significantly higher ($p<0.01$), and HDL-C levels were significantly lower ($P<0.01$) in the model group. Compared with the model group, the levels of TC, TG and LDL-C were significantly lower ($p<0.01$), and the levels of HDL-C were significantly higher ($p<0.01$) in the Bufrudin and rosuvastatin groups. These results indicated that Bufrudin improved lipid metabolism levels in ApoE-/- mice.

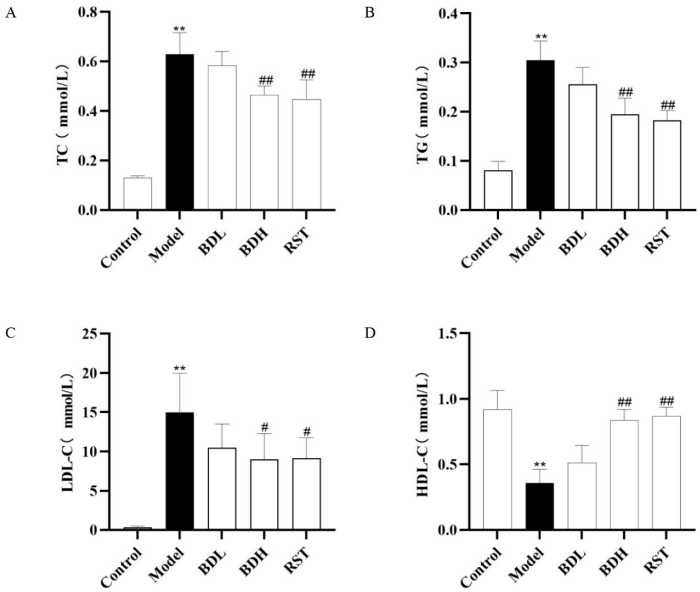

Fig. 1: Effects of Bufrudin on the serum lipid levels in ApoE-/- mice. (A): TC levels in mice blood lipids; (B): TG levels in mice blood lipids; (C): LDL-C levels in mice blood lipids and (D): HDL-C levels in mice blood lipids
Note: Data are expressed as mean±Standard Deviation (SD). **p<0.01 compared with the control group, #p<0.05 and ##p<0.01 compared with the model group

As shown in fig. 2A, Hematoxylin and Eosin (H&E) staining showed that the aortic wall layers of mice in the control group were structurally intact, the intima was intact and smooth, the smooth muscle cells were neatly arranged and the elastic fibres were arranged typically. Plaques and foam cells were present in the aorta of mice in the model group. Compared with the model group, the aortic lesions were reduced to different degrees in the high-dose and low-dose Bufrudin groups and in the rosuvastatin group.

Frozen sections of mouse aorta were stained with ORO, as shown in fig. 2B and fig. 2C. The AS plaque area/vessel area ratio (Splaque/Svessel) was significantly higher in the model group compared with the control group ($p<0.01$). The Splaque/Svessel ratio was significantly lower in the Bufrudin high-dose and rosuvastatin group compared with the model group ($p<0.01$). The Splaque/Svessel ratio was decreased in the Bufrudin low-dose group compared with the model group, but the difference was not statistically significant.

Masson's trichrome stain was used to detect the collagen content of aortic plaques in ApoE-/- mice. In Masson's trichrome stain, collagen in the plaques was blue-green, myofibrils and cytoplasm were red, and nuclei were blue-black. As shown in fig. 3, vascular collagen was normal and without fibrosis in the control group of mice. However, as shown in fig. 3B, compared with the control group, vascular collagen fibres in the model group of mice were abnormally proliferated, collagen fibrosis was severe and collagen was reduced to some extent. Compared with the model group, the intravascular collagen content was significantly increased in the Bufrudin high-dose group and the rosuvastatin group ($p<0.01$), and the intravascular collagen content was increased in the Bufrudin low-dose group compared with the model group, but the difference was not statistically significant.

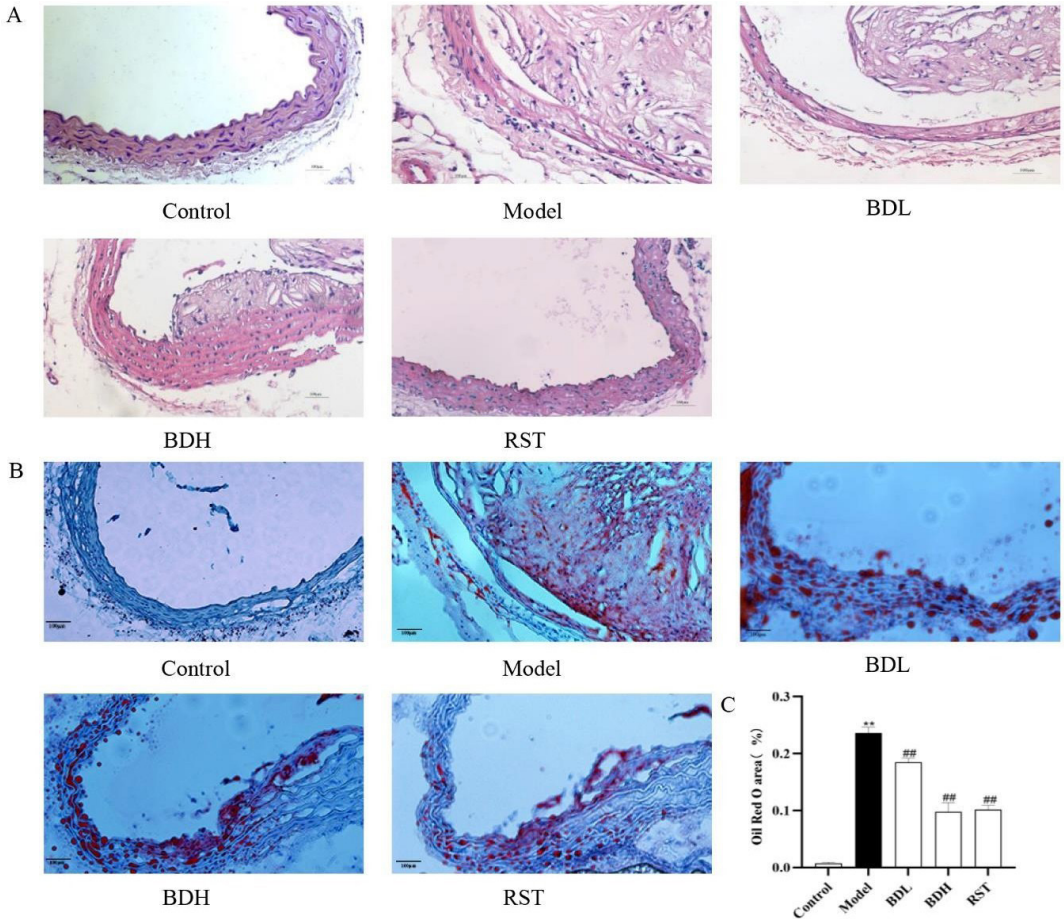

Fig. 2: Bufrudin improved the aorta of ApoE-/- mice in a dose-dependent manner. (A): Vascular morphology in each group of mice detected by H&E staining (magnification, X200); (B): Mouse aorta ORO staining results (magnification, X200) and (C): Effects of Bufrudin on the area of aortic plaques in mice

Note: All values were expressed as mean±SD, **$p<0.01$ compared with the blank control group and $^{\#}p<0.05$, $^{\#\#}p<0.01$ compared with the model group

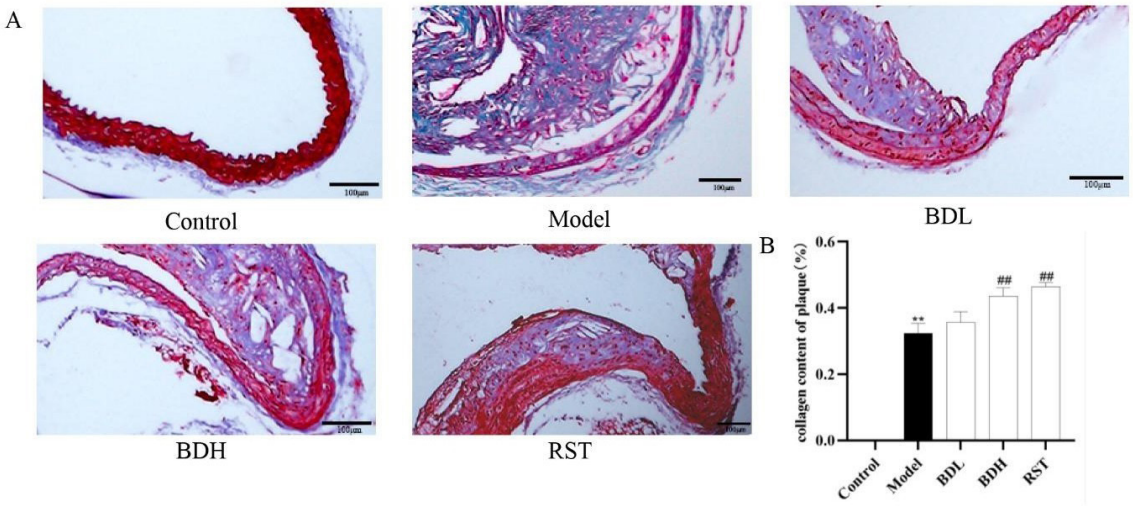

Fig. 3: Effect of Bufrudin on collagen content of aortic plaques in ApoE-/- mice. (A): Measurement of collagen contents by Masson's trichrome staining of the aorta (magnification, X200) and (B) effects of Bufrudin on aortic collagen fibers in mice
Note: All values were expressed as mean±SD, **p<0.01 compared with the blank control and #p<0.05, ##p<0.01 compared with the model group

ELISA kits were used to measure the concentrations of IL-6, TNF-α and CRP in the serum of mice from each group. As shown in fig. 4, compared with the control group, the model group exhibited a significant increase in concentrations of IL-6, TNF-α and CRP ($p<0.01$). In comparison with the model group, both the high-dose Bufrudin group and the rosuvastatin group demonstrated a significant decrease in IL-6 and TNF-α concentrations ($p<0.01$). In comparison with the model group, the low-dose Bufrudin group showed a reduction in CRP concentration, but the difference was not statistically significant ($p>0.05$). These results indicated that Bufrudin can ameliorate the inflammatory response in AS mice.

The expression of c-MYC, MEK3 and p38 MAPK proteins in the aortic vessels of ApoE-/- mice in each group were detected by Western blotting. As shown in fig. 5, c-MYC, MEK3 and p38 MAPK protein expression were significantly upregulated in the model group compared with the control group ($p<0.01$), and c-MYC, MEK3 and p38 MAPK protein expression was significantly downregulated in the Bufrudin group compared with the model group ($p<0.01$) with rosuvastatin. These data suggested that Bufrudin exerts its anti-AS effect by inhibiting the p38 MAPK signalling pathway.

RT-qPCR was performed to detect the expression level of mRNAs related to the NF-κB pathway by Bufrudin. As shown in fig. 6, mRNA expression of CD36, TLR-4, MyD88 and NF-κB in the aorta of mice in the model group was significantly elevated compared with that in the control group ($p<0.01$), and mRNA expression of CD36, TLR-4, MyD88 and NF-κB in the aorta of mice in the Bufrudin group was significantly decreased compared with that in the model group ($p<0.05$ or $p<0.01$) with respect to that in the rosuvastatin group. The aforementioned results suggested that Bufrudin can play an anti-AS role by inhibiting the expression of genes related to the NF-κB pathway.

Bufrudin attenuates AS in ApoE-/- mice by inhibiting the expression of NF-κB pathway-associated proteins: Immunohistochemistry was performed to detect the expression level of NF-κB pathway-related proteins by Bufrudin. As shown in fig. 7 and fig. 8, aortic CD36, TLR4, MyD88 and NF-κB protein expression was not significant in the control group of mice, and aortic CD36, TLR4, MyD88 and NF-κB protein expression was significantly increased in the model group of mice compared with the control group ($p<0.01$). Furthermore, aortic CD36, TLR4, MyD88 and NF-κB protein expression was significantly decreased in the Bufrudin and rosuvastatin group compared with the model group, and in the rosuvastatin group, TLR4, MyD88 and NF-κB proteins were significantly lower in the Bufrudin group compared with the model group. These results suggested that Bufrudin can play an anti-AS role by inhibiting the expression of NF-κB pathway-related proteins.

AS is a disease of chronic progressive lipid deposition, inflammatory response and focal thickening of fibrous tissue occurring mainly in large and medium-sized arterial vessels[1]. Among other

things, inflammation can promote the rupture of vulnerable plaques, leading to thrombotic occlusion of coronary and cerebral arteries and ultimately the onset of heart disease or stroke, which are leading causes of death worldwide[2]. Therefore, searching for drugs that can effectively treat or prevent AS is crucial.

Lipids are an essential factor affecting the development of AS, and cholesterol, triglyceride and lipoprotein levels are closely related to the development of AS. Long term elevation of blood lipids tends to cause cholesterol to invade the walls of large blood vessels, and deposit and accumulate to promote the proliferation of arterial smooth muscle cells and fibroblasts[3,4]. With the elevation of blood lipids, a large number of proteins such as LDL-C, Apolipoprotein B (ApoB) and other proteins are deposited in the arterial wall. Furthermore, LDL is oxidized to ox-LDL thus causing a series of pathological changes. In addition, elevated serum LDL-C and TG are significant causes of AS formation[5], of which LDL-C is the most critical[6,7]. Retention of LDL particles in the vessel wall is considered to be the first step in the pathogenesis of AS[8]. When levels of oxidative stress increase, LDL becomes oxidized and modified by ApoB to become a scavenger ligand. This ligand can be recognized and phagocytosed by CD36 on macrophages, forming foam cells and promoting AS lesions[9]. The 2019 European Society of Cardiology/European AS Society emphasizes minimizing LDL-C levels to prevent AS and other CVDs[10]. Currently, statins play a role in treating AS by promoting AS plaque stabilization and reducing coronary plaque volume, primarily by lowering LDL-C levels[11,12,17]. In the present study, Bufrudin significantly reduced LDL-C, TG and TC serum levels and increased HDL-C serum levels in the AS model mice. These data suggested that Bufrudin can exert anti-AS effects by improving lipid levels in an AS mouse model.

Despite current advancements in AS treatments, further research into the prevention of AS is required[18]. Numerous studies have confirmed plaque formation and rupture as a hallmark of AS disease[18,27]. In the present study, the ORO and H&E staining results showed that arterial plaques were evident in the model group, whereas arterial plaque was significantly improved in both the Bufrudin and rosuvastatin groups compared with the model group. These results suggested that Bufrudin can improve AS symptoms in mice. The inflammatory response not only promotes the production of inflammatory factors such as IL-6, IL-7 and TNF-α but also promotes the development of AS[1]. A large body of evidence confirms that typical pro-inflammatory cytokines, such as TNF-α and IL-6, are considered to play critical roles in inflammatory pathophysiologic disorders and are involved in inducing and maintaining the development of AS. For example, elevated TNF-α can lead to macrophage activation, which results in the uptake of large amounts of ox-LDL, ultimately forming foam cells, which in turn induces the formation of AS plaques[19]. CRP is considered a predictor of cardiovascular event occurrence and a downstream marker of IL-6 and TNF-α[20], synthesized in the liver induced by IL-6 and TNF-α. CRP levels, on the other hand, are dramatically increased during bacterial infections, trauma, tissue necrosis and most types of inflammatory response[21], and in programmed injury cardiomyocytes or visibly necrotic muscle fibers[22]. It has also been demonstrated that overexpression of CRP, a marker of arterial stiffness, leads to elevated levels of arterial Elastance (Ea), which further promotes the development of AS[28]. As hypothesized, in the present study, the serum levels of TNF-α, IL-6 and CRP were significantly higher in the model group of mice than in the normal group, whereas the serum levels of TNF-α, IL-6 and CRP were significantly lower in the Bufrudin and rosuvastatin groups than in the model group. These data suggested that Bufrudin can exert an ameliorative effect on AS by inhibiting the inflammatory response.

There is increasing evidence that the p38 MAPK signalling pathway plays a crucial role in AS. It can activate the production of multiple inflammatory factors, regulate the activity of transcription factors, alter mitochondrial membrane potential, affect cysteine proteases and promote smooth muscle cell apoptosis, thus exacerbating the progression of AS through multiple pathways[29]. MEK3, as an upstream regulator of the p38 MAPK signalling pathway, can activate p38 through Thr180 and Tyr182 to activate p38[30,31]. There is increasing evidence that the MEK3/p38 MAPK pathway is involved in the expression of numerous inflammatory mediators[32], and that the activation of its pathway is closely associated with AS, endothelial dysfunction, VSMC cellular hypertrophy and aortic valve sclerosis[33]. There have been relevant studies confirming that

by inhibiting the MEK3/p38 MAPK pathway, the MEK3/p38 MAPK pathway can be activated[34,35]. The p38 MAPK pathway can inhibit ox-LDL-induced inflammatory responses in macrophages. Furthermore, it has been demonstrated that MAPK is involved in cardiac vasodilatation[36], and that the p38 MAPK pathway can be inhibited by downregulation of MEK3 expression, thereby inhibiting the development of coronary AS[37,38]. c-MYC is also an upstream regulator in the p38 MAPK pathway and is involved in initiating the early oxidative sensitization mechanism of AS in both *in vivo* and *in vitro* experiments. Studies have identified the presence of c-MYC[39], which is involved in initiating oxidative sensitization mechanisms, in early AS in *in vivo* and *in vitro* experiments[40,41]. Other studies have shown that the downregulation of c-MYC expression inhibits the proliferation of human VSMC[42]. Among the current anti-AS perspectives, the downregulation of c-MYC by antioxidants has been recognized as a promising pharmacological therapeutic approach for vascular diseases[39,40,43]. Notably, in the present study, Bufrudin downregulated the expression of c-MYC, MEK3 and p38 MAPK proteins in the AS mouse model, suggesting that Bufrudin is capable of treating AS by inhibiting the expression of proteins related to the p38 MAPK pathway.

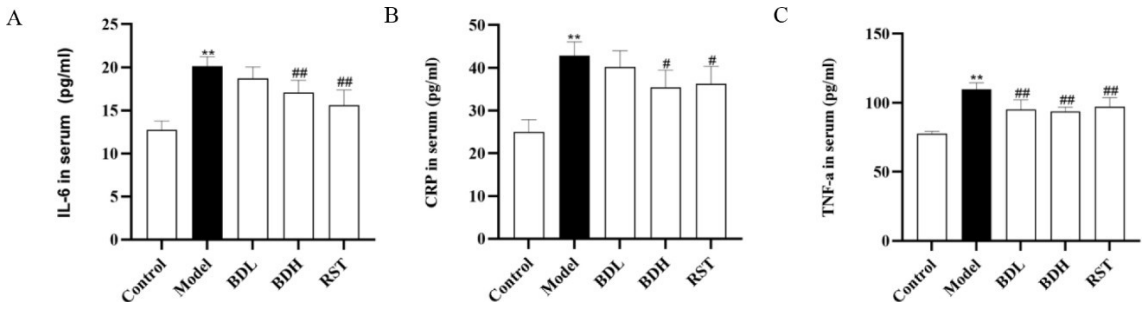

Fig. 4: Effects of Bufrudin on the serum contents of IL-6, TNF-α and CRP in mice. (A): Levels of IL-6 in mouse serum; (B): Levels of TNF-α in mouse serum and (C): Levels of CRP in mouse serum
Note: All values were expressed as mean±SD. **p<0.01 compared with the blank control group and #p<0.05, ##p<0.01 compared with the model group

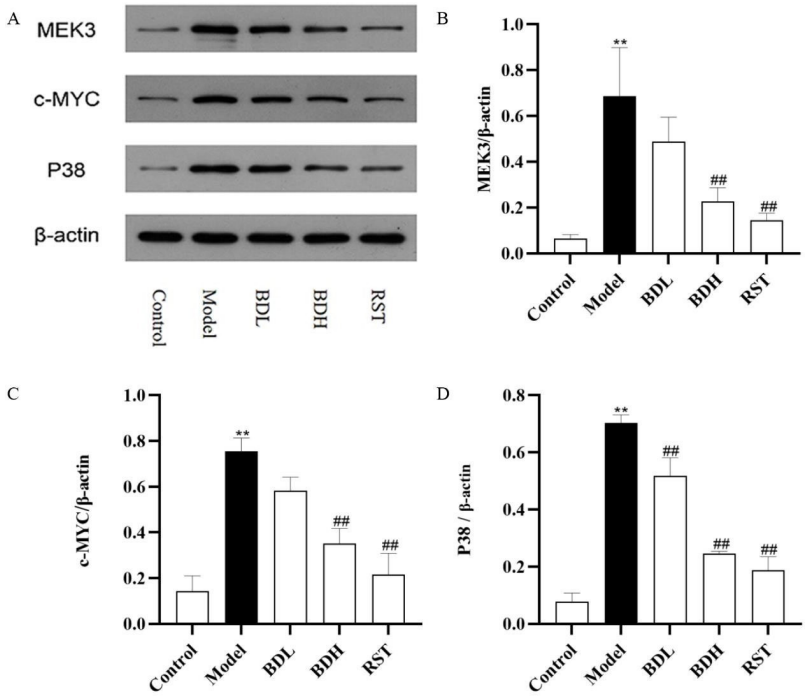

Fig. 5: Expression of c-MYC, MEK3 and p38 MAPK proteins in ApoE-/- mice were detected by Western blotting. (A): Assessment and statistical analysis of protein levels in the p38 MAPK pathway; (B): Relative expression level of MEK3 protein; (C): Relative expression level of c-MYC protein and (D): Relative expression level of p38 MAPK protein
Note: Data were expressed as mean±SD. **p<0.01 compared with the blank control group and #p<0.05, ##p<0.01 compared with the model group

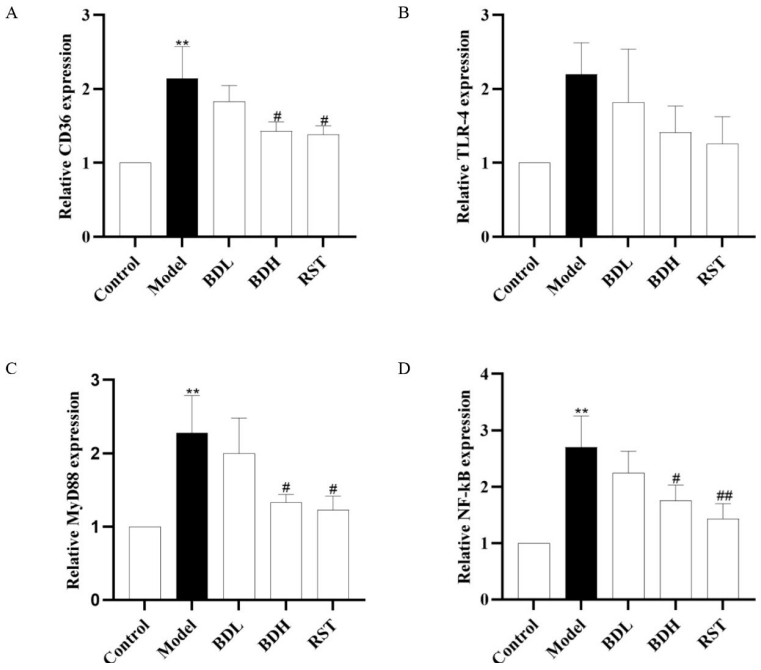

Fig. 6: RT-qPCR was performed to detect the expression level of mRNAs related to the NF-κB pathway by Bufrudin. (A): Relative expression of CD36 mRNA; (B): Relative expression of TLR4 mRNA; (C): Relative expression of MyD88 mRNA and (D): Relative expression of NF-κB mRNA

Note: Data were expressed as mean±SD. **p<0.01 compared with the blank control group and #p<0.05, ##p<0.01 compared with the model group

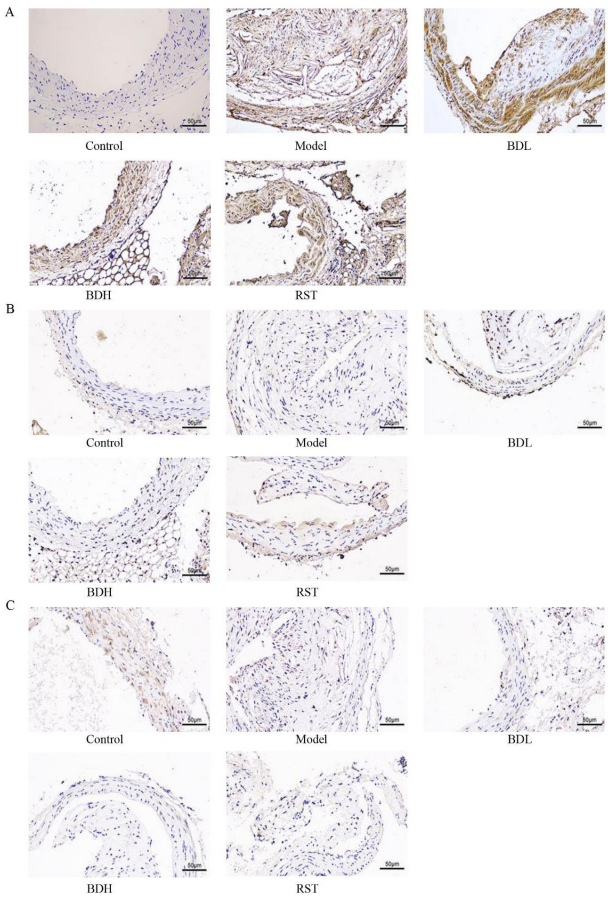

Fig. 7: Effects of Bufrudin on the NF-κB pathway-related protein expression. (A): Immunohistochemical staining of CD36 protein in mouse aortas treated with Bufrudin; (B): Immunohistochemical staining of TLR4 protein in mouse aortas treated with Bufrudin and (C): Immunohistochemical staining of MyD88 protein in mouse aortas treated with Bufrudin

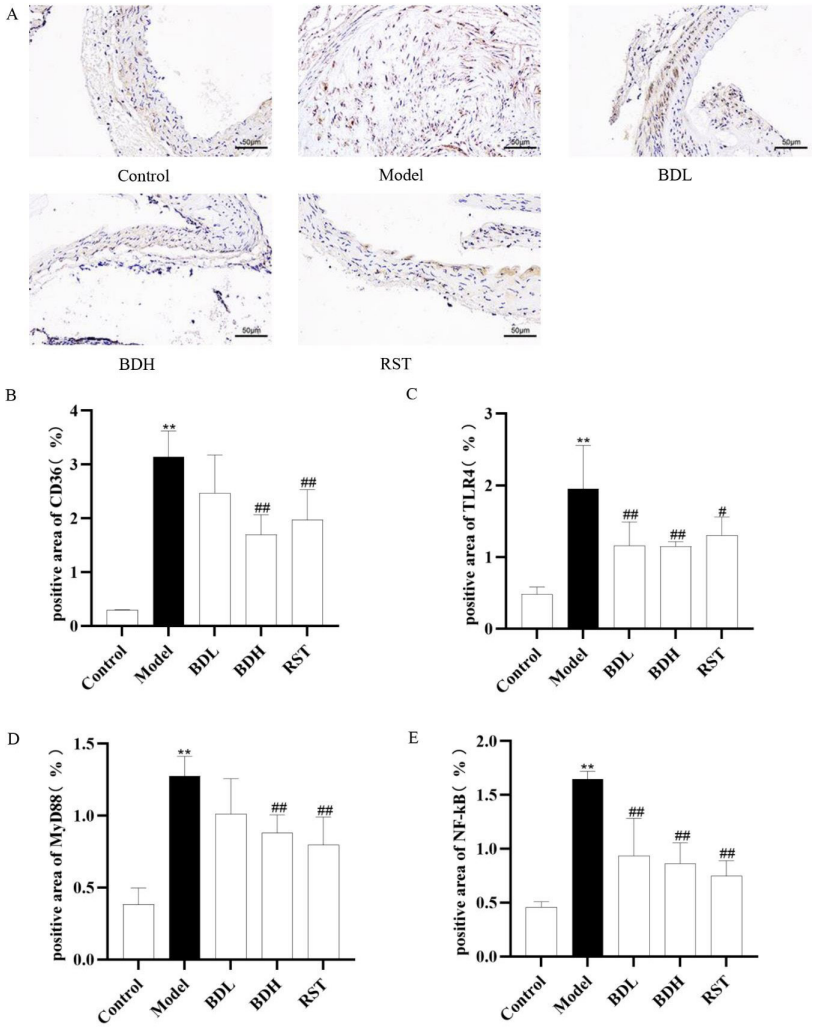

Fig. 8: Effects of Bufrudin on NF-κB pathway-related protein expression. (A): Immunohistochemical staining of NF-κB protein in mouse aortas treated with Bufrudin; (B): Positive area of CD36; (C) Positive area of TLR4; (D): Positive area of MyD88 and (E): Positive area of NF-κB.

Note: All values were expressed as means±SD. **p<0.01 compared with the blank control group and #p<0.05, ##p<0.01 compared with the model group

Inhibition of TLR4/MyD88/NF-κB signalling pathway activation is a promising therapeutic strategy for AS[44]. TLR4 is a specific member of the TLR family, widely present in CVDs and cancers[45,46]. It has been shown that TLR4 plays an important role in innate immunity and the inflammatory response to exogenous and endogenous stimuli by upregulating relevant inflammatory factors[47]. Activation of TLR4 not only increases ox-LDL uptake and foam cell formation but also activates its mediated production of pro-inflammatory cytokines by NF-κB transcription factors, which affects cholesterol metabolism as well as promotes the expression of relevant pro-inflammatory cytokines, such as TNF-α, GM-CSF and IL-1α/β to trigger the inflammatory response and promote the accumulation of endothelial foam cells[48]. MyD88 is an intracellular adaptor protein that orchestrates a cascade of pro-inflammatory signalling, with most TLRs, as well as other related cytokine receptors, signalling through MyD88[49,50]. The activation of MyD88 leads to the activation of inflammatory pathways such as NF-κB[51]. It has been demonstrated that TLR4/MyD88 signalling is involved in macrophage phagocytosis of lipids and plaque foam cell formation[52], and that aberrant activation of TLRs and MyD88 is present during AS lesions in both humans and mice[53]. Notably, MyD88 downregulation reduces aortic AS development and macrophage accumulation in ApoE-/- mice, and overall deletion of TLRs and MyD88 are beneficial for ameliorating AS plaques[54]. Both the NF-κB and p38 MAPK pathways are vital regulatory points in AS Some studies have shown that inhibition of NF-κB reduces inflammatory lesions[55,56]. Other studies

demonstrated that endothelial-specific deletion of relevant signalling molecules in the NF-κB pathway significantly reduces AS lesions in ApoE-/- mice[13,57]. CD36 is a key member of the class B scavenger receptor family[58], and when CD36 binds to various types of ligands, it initiates intracellular signalling, thereby promoting angiogenesis, inflammation and the development of AS[59]. Increasing evidence suggested that inhibition of CD36 expression can exert anti-AS effects[60,61]. For example, in chronic inflammation, oxidative stress and hyperlipidaemia, the reduction of CD36 has a profound preventive and protective effect on AS and thrombosis and can significantly ameliorate the progression of AS in ApoE-/- mice[62]. In the present study, it was shown that Bufrudin reduced the expression of CD36, TLR4, MyD88 and NF-κB mRNA in the aorta of an AS mouse model by RT-qPCR. Immunohistochemistry results further revealed that Bufrudin was able to reduce the expression of CD36, TLR4, MyD88 and NF-κB proteins in the aorta of an AS mouse model, suggesting that Bufrudin could play a therapeutic role in AS by inhibiting the TLR4/ NF-κB pathway.

The present study had several limitations. First, *in vitro* experiments involving smooth muscle cells or macrophages cells were not carried out. Second, due to limited time and funding, the exploration of all underlying mechanisms was not undertaken. Finally, other potential targets and pathways influenced by Bufrudin were not extensively investigated. These limitations will be addressed in future studies involving Bufrudin.

To conclude, the results of the present study suggested that Bufrudin achieves therapeutic effects in AS by improving lipid levels, inhibiting inflammatory responses and increasing aortic collagen content in mice, which in turn inactivates the TLR4/NF-κB/p38 MAPK signalling pathway. These results provide new insights into how Bufrudin ameliorates AS, suggesting that Bufrudin may be a potential adjunctive therapeutic agent for treating CVDs.

Funding:

This research was funded by the Guangxi Natural Science Foundation, China (2020GXNSFAA238042).

Authors' contributions:

Jixing Li: Methodology, Software, Formal analysis, Experiment, Writing-original draft, Writing-review and editing, Visualization; Wenxing Wei: Methodology, Project administration, Supervision, Writing-review & editing; Si Lin: Writing-review & editing; Wenwen Tan: Formal analysis Data Curation; Zongqiang Lai: Investigation; Yu Tu: Investigation and Yuanhong Li: Conceptualization, Methodology, Project administration, Resources, Writing-review & editing, funding acquisition, Supervision. All authors have read and agreed to the published version of the manuscript. Jixing Li, Wenxing Wei first two authors equally to this work.

Ethics approval:

This experiment was approved and agreed by The Animal Care and Welfare Committee of Guangxi Medical University (Certificate No.: SYXK Gui 2020-0004).

Conflict of interests:

The authors declared no conflict of interests.

REFERENCES

1. Fan Q, Liu Y, Rao J, Zhang Z, Xiao W, Zhu T, *et al*. Anti-atherosclerosis effect of Angong Niuhuang Pill *via* regulating Th17/Treg immune balance and inhibiting chronic inflammatory on ApoE-/-mice model of early and mid-term atherosclerosis. Front Pharmacol 2020;10:1584.
2. Major AS, Fazio S, Linton MF. B-lymphocyte deficiency increases atherosclerosis in LDL receptor-null mice. Arterioscler Thromb Vasc Biol 2002;22(11):1892-8.
3. Zhao S, Zhong J, Sun C, Zhang J. Effects of aerobic exercise on TC, HDL-C, LDL-C and TG in patients with hyperlipidemia: A protocol of systematic review and meta-analysis. Medicine 2021;100(10):e25103.
4. Firdous SM, Hazra S, Gopinath SC, El-Desouky GE, Aboul-Soud MA. Antihyperlipidemic potential of diosmin in Swiss Albino mice with high-fat diet induced hyperlipidemia. Saudi J Biol Sci 2021;28(1):109-15.
5. Albertini R, Moratti R, Luca G. Oxidation of low-density lipoprotein in atherosclerosis from basic biochemistry to clinical studies. Curr Mol Med 2002;2(6):579-92.
6. Ference BA, Ginsberg HN, Graham I, Ray KK, Packard CJ, Bruckert E, *et al*. Low-density lipoproteins cause atherosclerotic cardiovascular disease. Evidence from genetic, epidemiologic, and clinical studies. A consensus statement from the European Atherosclerosis Society Consensus Panel. Eur Heart J 2017;38(32):2459-72.
7. Boren J, Chapman MJ, Krauss RM, Packard CJ, Bentzon JF, Binder CJ, *et al*. Low-density lipoproteins cause atherosclerotic cardiovascular disease: Pathophysiological, genetic, and therapeutic insights: A consensus statement from the European Atherosclerosis Society Consensus Panel. Eur Heart J 2020;41(24):2313-30.
8. Wiśniewska A, Olszanecki R, Totoń-Żurańska J, Kuś K, Stachowicz A, Suski M, *et al*. Anti-atherosclerotic action of agmatine in ApoE-knockout mice. Int J Mol Sci 2017;18(8):1706.
9. Zhou MS, Chadipiralla K, Mendez AJ, Jaimes EA, Silverstein RL, Webster K, *et al*. Nicotine potentiates proatherogenic effects of oxLDL by stimulating and

upregulating macrophage CD36 signaling. Am J Physiol Heart Circ Physiol 2013;305(4):H563-74.
10. Mach F, Baigent C, Catapano AL, Koskinas KC, Casula M, Badimon L, *et al*. 2019 ESC/EAS Guidelines for themanagement of dyslipidaemias: Lipid modification to reduce cardiovascular risk. Russian J Cardiol 2020;25(5):3826.
11. Tang X, Yang Y, Luo S, Zhao Y, Lu C, Luo Y, *et al*. The effect of statin therapy on plaque regression following acute coronary syndrome: A meta-analysis of prospective trials. Coron Artery Dis 2016;27(8):636-49.
12. Nicholls SJ, Tuzcu EM, Sipahi I, Grasso AW, Schoenhagen P, Hu T, *et al*. Statins, high-density lipoprotein cholesterol, and regression of coronary atherosclerosis. JAMA 2007;297(5):499-508.
13. Karunakaran D, Nguyen MA, Geoffrion M, Vreeken D, Lister Z, Cheng HS, *et al*. RIPK1 expression associates with inflammation in early atherosclerosis in humans and can be therapeutically silenced to reduce NF-κB activation and atherogenesis in mice. Circulation 2021;143(2):163-77.
14. Zheng Y, Li Y, Ran X, Wang D, Zheng X, Zhang M, *et al*. Mettl14 mediates the inflammatory response of macrophages in atherosclerosis through the NF-κB/IL-6 signaling pathway. Cell Mol Life Sci 2022;79(6):311.
15. Chinetti-Gbaguidi G, Colin S, Staels B. Macrophage subsets in atherosclerosis. Nat Rev Cardiol 2015;12(1):10-7.
16. McArdle S, Buscher K, Ghosheh Y, Pramod AB, Miller J, Winkels H, *et al*. Migratory and dancing macrophage subsets in atherosclerotic lesions. Circ Res 2019;125(12):1038-51.
17. Matsushita K, Hibi K, Komura N, Akiyama E, Maejima N, Iwahashi N, *et al*. Effects of 4 statins on regression of coronary plaque in acute coronary syndrome. Circ J 2016;80(7):1634-43.
18. Stefanadis C, Antoniou CK, Tsiachris D, Pietri P. Coronary atherosclerotic vulnerable plaque: Current perspectives. J Am Heart Assoc 2017;6(3):e005543.
19. Geng YJ, Kodama T, Hansson GK. Differential expression of scavenger receptor isoforms during monocyte-macrophage differentiation and foam cell formation. Arterioscler Thromb 1994;14(5):798-806.
20. Kaptoge S, Di Angelantonio E, Pennells L, Wood AM, White IR, Gao P, *et al*. C-reactive protein, fibrinogen, and cardiovascular disease prediction. N Engl J Med 2012;367(14):1310-20.
21. Pepys MB. C-reactive protein fifty years on. Lancet 1981;317(8221):653-7.
22. Pepys MB, Rowe IF, Baltz ML. C-reactive protein: Binding to lipids and lipoproteins. Int Rev Exp Pathol 1985;27:83-111.
23. Abdualkader AM, Ghawi AM, Alaama M, Awang M, Merzouk A. Leech therapeutic applications. Indian J Pharm Sci 2013;75(2):127.
24. Wang Y, Zhao X, Wang YS, Song SL, Liang H, Ji AG. An extract from medical leech improve the function of endothelial cells *in vitro* and attenuates atherosclerosis in ApoE null mice by reducing macrophages in the lesions. Biochem Biophysic Res Commun 2014;455(1-2):119-25.
25. Lai W, Zhou W, Huang L, Li Y. Interventional effects of Bufrudin on atherosclerosis plaque in ApoE gene knockout mice. Chin Acad J Electron Publ House 2017;33:4.
26. Huang L. Effect of Bufrudin on atherosclerosis in APOE-knockout mice. Journal 2018
27. Hafiane A. Vulnerable plaque, characteristics, detection, and potential therapies. J Cardiovasc Dev Dis 2019;6(3):26.
28. Kelly RP, Ting CT, Yang TM, Liu CP, Maughan WL, Chang MS, *et al*. Effective arterial elastance as index of arterial vascular load in humans. Circulation 1992;86(2):513-21.
29. Schindler JF, Monahan JB, Smith WG. p38 pathway kinases as anti-inflammatory drug targets. J Dental Res 2007;86(9):800-11.
30. Zarubin T, Han J. Activation and signaling of the p38 MAP kinase pathway. Cell Res 2005;15(1):11-8.
31. Niaudet C, Bonnaud S, Guillonneau M, Gouard S, Gaugler MH, Dutoit S, *et al*. Plasma membrane reorganization links acid sphingomyelinase/ceramide to p38 MAPK pathways in endothelial cells apoptosis. Cell Signal 2017;33:10-21.
32. Yang Y, Kim SC, Yu T, Yi YS, Rhee MH, Sung GH, *et al*. Functional roles of p38 mitogen-activated protein kinase in macrophage-mediated inflammatory responses. Mediators Inflamm 2014;2014(1):352371.
33. Reustle A, Torzewski M. Role of p38 MAPK in atherosclerosis and aortic valve sclerosis. Int J Mol Sci 2018 Nov 27;19(12):3761.
34. Zhai C, Cong H, Hou K, Hu Y, Zhang J, Zhang Y, *et al*. Effects of miR-124-3p regulation of the p38MAPK signaling pathway *via* MEKK3 on apoptosis and proliferation of macrophages in mice with coronary atherosclerosis. Adv Clin Exp Med 2020;29(7):803-12.
35. Ren R, Chen SD, Fan J, Zhang G, Li JB. miRNA-138 regulates MLK3/JNK/MAPK pathway to protect BV-2 cells from H2O2-induced apoptosis. Bratisl Lek Listy 2018;119(5):284-8.
36. Feng H, Cao J, Zhang G, Wang Y. Kaempferol attenuates cardiac hypertrophy *via* regulation of ASK1/MAPK signaling pathway and oxidative stress. Planta Med 2017;83(10):837-45.
37. Padda R, Wamsley-Davis A, Gustin MC, Ross R, Yu C, *et al*. MEKK3-mediated signaling to p38 kinase and TonE in hypertonically stressed kidney cells. Am J Physiol Renal Physiol 2006;291(4):F874-81.
38. Xu J, Tang S, Yin B, Sun J, Bao E. Co-enzyme Q10 upregulates Hsp70 and protects chicken primary myocardial cells under *in vitro* heat stress *via* PKC/MAPK. Mol Cell Biochem 2018;449:195-206.
39. Napoli C, Lermant LO, De Nigris F, Sica V. c-Myc oncoprotein: A dual pathogenic role in neoplasia and cardiovascular diseases?. Neoplasia 2002;4(3):185-90.
40. de Nigris F, Lerman LO, Rodriguez-Porcel M, de Montis MP, Lerman A, Napoli C. C-myc activation in early coronary lesions in experimental hypercholesterolemia. Biochem Biophys Res Commun 2001;281(4):945-50.
41. Sagun KC, Cárcamo JM, Golde DW. Antioxidants prevent oxidative DNA damage and cellular transformation elicited by the over-expression of c-MYC. Mutat Res 2006;593(1-2):64-79.
42. Nigris FD, Balestrieri ML, Napoli C. Targeting c-Myc, Ras and IGF cascade to treat cancer and vascular disorders. Cell Cycle 2006;5(15):1621-8.
43. Secombe J, Pierce SB, Eisenman RN. Myc: A weapon of mass destruction. Cell 2004;117(2):153-6.
44. Li Y, Zhang L, Ren P, Yang Y, Li S, Qin X, *et al*. Qing-Xue-Xiao-Zhi formula attenuates atherosclerosis by inhibiting macrophage lipid accumulation and inflammatory response *via* TLR4/MyD88/NF-κB pathway regulation.

Phytomedicine 2021;93:153812.
45. Ferronato S, Scuro A, Fochi S, Orlandi E, Gomez-Lira M, Olivato S, *et al*. Expression of TLR4-PTGE2 signaling genes in atherosclerotic carotid plaques and peripheral blood. Mol Biol Rep 2019;46(1):1317-21.
46. Chen CY, Kao CL, Liu CM. The cancer prevention, anti-inflammatory and anti-oxidation of bioactive phytochemicals targeting the TLR4 signaling pathway. Int J Mol Sci 2018;19(9):2729.
47. Gargiulo S, Gamba P, Testa G, Rossin D, Biasi F, Poli G, *et al*. Relation between TLR4/NF-κB signaling pathway activation by 27-hydroxycholesterol and 4-hydroxynonenal, and atherosclerotic plaque instability. Aging Cell 2015;14(4):569-81.
48. Xu XH, Shah PK, Faure E, Equils O, Thomas L, Fishbein MC, *et al*. Toll-like receptor-4 is expressed by macrophages in murine and human lipid-rich atherosclerotic plaques and upregulated by oxidized LDL. Circulation 2001;104(25):3103-8.
49. Cohen P. The TLR and IL-1 signalling network at a glance. J Cell Sci 2014;127(11):2383-90.
50. Deguine J, Barton GM. MyD88: A central player in innate immune signaling. F1000prime Rep 2014;6:97.
51. Bayer AL, Alcaide P. MyD88: At the heart of inflammatory signaling and cardiovascular disease. J Mol Cell Cardiol 2021;161:75-85.
52. Bjorkbacka H, Kunjathoor VV, Moore KJ, Koehn S, Ordija CM, Lee MA, *et al*. Reduced atherosclerosis in MyD88-null mice links elevated serum cholesterol levels to activation of innate immunity signaling pathways. Nature Med 2004;10(4):416-21.
53. Cai S, Batra S, Shen L, Wakamatsu N, Jeyaseelan S. Both TRIF-and MyD88-dependent signaling contribute to host defense against pulmonary *Klebsiella* infection. J Immunol 2009;183(10):6629-38.
54. Michelsen KS, Wong MH, Shah PK, Zhang W, Yano J, Doherty TM, *et al*. Lack of Toll-like receptor 4 or myeloid differentiation factor 88 reduces atherosclerosis and alters plaque phenotype in mice deficient in apolipoprotein E. Proc Natl Acad Sci 2004;101(29):10679-84.
55. Baker RG, Hayden MS, Ghosh S. NF-κB, inflammation, and metabolic disease. Cell Metab 2011;13(1):11-22.
56. Back M, Hansson GK. Anti-inflammatory therapies for atherosclerosis. Nat Rev Cardiol 2015;12(4):199-211.
57. Mallavia B, Recio C, Oguiza A, Ortiz-Muñoz G, Lazaro I, Lopez-Parra V, *et al*. Peptide inhibitor of NF-κB translocation ameliorates experimental atherosclerosis. Ame J Pathol 2013;182(5):1910-21.
58. Jay AG, Hamilton JA. The enigmatic membrane fatty acid transporter CD36: New insights into fatty acid binding and their effects on uptake of oxidized LDL. Prostaglandins Leukot Essent Fatty Acids 2018;138:64-70.
59. Han S, Sidell N. Peroxisome-proliferator-activated-receptor gamma (PPARγ) independent induction of CD36 in THP-1 monocytes by retinoic acid. Immunology 2002;106(1):53-9.
60. Lin HC, Lii CK, Chen HC, Lin AH, Yang YC, Chen HW. Andrographolide inhibits oxidized LDL-induced cholesterol accumulation and foam cell formation in macrophages. Am J Chin Med 2018;46(01):87-106.
61. Li ZM, Xu SW, Liu PQ. *Salvia miltiorrhiza* Burge (Danshen): A golden herbal medicine in cardiovascular therapeutics. Acta Pharmacol Sin 2018;39(5):802-24.
62. Podrez EA, Byzova TV, Febbraio M, Salomon RG, Ma Y, Valiyaveettil M, *et al*. Platelet CD36 links hyperlipidemia, oxidant stress and a prothrombotic phenotype. Nat Med 2007;13(9):1086-95.